

Experimental study of precipitating systems; computerised analysis of the optical transmittance and associated noise

J.A. Poce-Fatou *, R. Alcántara, J.J. Gallardo, J. Martín

Departamento de Química Física, Facultad de Ciencias, Universidad de Cádiz, Apartado nº 40, 11510 Puerto Real, Cádiz, Spain

Received 17 August 2000; received in revised form 4 September 2000; accepted 9 October 2000

Abstract

The change of the transmittance in a precipitant system has been measured by using a focused laser beam into a precipitation cell in which the precipitate was generated by an injection technique. We have monitored the evolution of the transmittance on several precipitation processes with different chemicals (PbI_2 , PbSO_4 , BaSO_4 and BaC_2O_4) and quantities of precipitated mass (20.0, 17.5, 15.0, 12.5 and 10.0 mg). The noise associated to the transmittance signal has been obtained by a numerical procedure based on computer analysis, finding that it provides information about particle shape features and nucleation kinetics. © 2001 Elsevier Science Ltd. All rights reserved.

Keywords: Precipitation; Noise; Transmittance; Computerised analysis

1. Introduction

The use of lasers in chemistry has spread widely in the last years, finding multiple applications. In the study of precipitant systems, the measurement of the intensity of a transmitted laser beam is used as a technique for measuring transmittances (Carton et al., 1999). However, not only the measurement of the intensities is of value in this field. The study of the associated noise also involves an interesting contribution. In this way, several laser techniques have been used for the detection of the salting-out in precipitant systems (Martín et al., 1991).

Two of these techniques are of special interest to us and have provided a basis for the present study. In the first of these techniques, a cylindrical path laser beam, crosses the reservoir where a precipitation process is being induced. In the second one, the laser beam is focused in the centre of that precipitant system. In both

methods, photodetectors are used for measuring the transmittance of the medium.

In the former, the salting-out was measured as the point where the transmittance signal started to decrease. In the latter, it was detected earlier, as the point where a large increase of the noise associated to the transmittance was observed.

The circular cross section of the cylindrical path is much larger than the particles' size, however the cross section of the focused path takes a size in the same order. In this way, in the cylindrical path small variations of the transmittance will remain masked by a mean value, while in a focused path these variations will magnify the noise of the transmittance. This fact decided us to favour the study of the noise in focused paths against cylindrical paths.

A focused laser beam constitutes a sensitive probe whose values could provide information related to the individual behaviour of the precipitated particles. Literature on the relationship between transmittance and nature of the precipitant systems (Martín et al. 1992; Mucha and Ganicz, 1996; Ohshima, 1996; Burger et al., 1997; Matthews and Rawlings, 1998), rarely makes any

* Corresponding author. Tel.: +34-956-016178; fax: +34-956-016288.

E-mail address: juanantonio.poce@uca.es (J.A. Poce-Fatou).

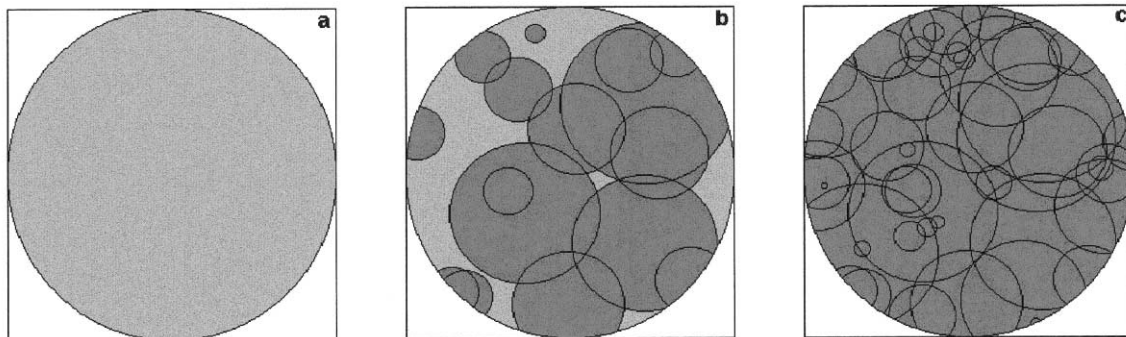


Fig. 1. Hypothetical evolution of the light projection on a photodetector during a precipitation process. Spherical morphology for particles is assumed.

reference to theoretical developments, paying little attention to the associated noise.

This paper tries to fill this vacuum and set the theoretical bases of a method for the study of precipitant systems based on the interpretation of the noise associated to the transmittance measured by using focused laser beams.

2. Material and methods

2.1. Theory

A laser working at the lowest order mode, TEM_{00} , has a cylindrical Gaussian irradiance distribution even when the beam is focused. The radius at which the transverse field amplitude has fallen to a fraction $1/e$ of its peak axial value is the Gaussian radius. At this same distance, the corresponding beam irradiance (intensity) will have fallen to $1/e^2$ (13.5%) of its peak or axial value (Gerrard and Burch, 1994).

In a focused path, the Gaussian radius of the focus can be calculated by,

$$R_0 = \frac{\lambda}{\pi} \cdot \frac{f_d}{r} \quad (1)$$

where λ is the radiation wavelength, f_d is the lens focal length and r is the prefocused Gaussian radius of the beam.

The Gaussian radius at any position of the path can be calculated by the hyperbolic function,

$$R_y = \pm R_0 \cdot \sqrt{1 + \left(\frac{\lambda}{\pi} \cdot \frac{y}{R_0^2} \right)^2} \quad (2)$$

where, y is the coordinate in the propagation axis.

The proper selection of the wavelength, focal length and prefocused radius of the beam makes possible to obtain R_0 values of just a few micrometers, which converts the laser beam into a probe for the on-line detection of opaque particles with a size in the order of R_0 .

The transmittance of a system can be defined as the ratio between irradiances,

$$\frac{I_t}{I_0} \quad (3)$$

where I_t is the intensity of the laser beam measured at time t and I_0 , is the intensity of the laser beam measured when the precipitation process has not started.

If we consider variations of the transmittance to be caused by opaque precipitated particles, we can describe a precipitation process in theoretical terms as follows,

1. Initial stages. There are no precipitated particles in the reservoir and there are no eclipsing phenomena. Transmittance is stabilised to its maximum value (Fig. 1a), while the electronic features of the instrumentation (photodetectors, amplifiers, laser stability, etc) are the only causes of fluctuations in the signal.
2. The precipitation process has started. The system evolves while particles change positions and orientations in a homogeneous stirred media, causing a decrease in the transmittance (Fig. 1b). The fluctuations caused by the dynamics of the particles increase the noise of the signal.
3. The precipitation is at its last stages. There is a large quantity of precipitated mass, which eclipses the laser beam totally. The transmittance reaches a minimum, which depends on the real opacity of the particles. The associated noise decreases to the levels of the electronic one (Fig. 1c).
4. As an evolution of the system after reaching minimum values of transmittance, we can consider the possibility of redistributions in the precipitated mass, in such a way, that it could be possible to detect changes in the number and size of particles which would entail an increasing transmittance. The growing of particles at the expense of their number fits with the stage shown in Fig. 1b.

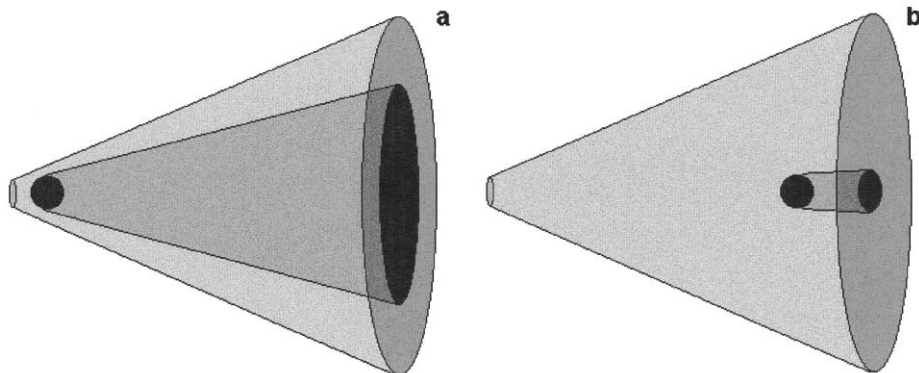


Fig. 2. Projection effect caused by a spherical particle placed in different positions into the post-focused path.

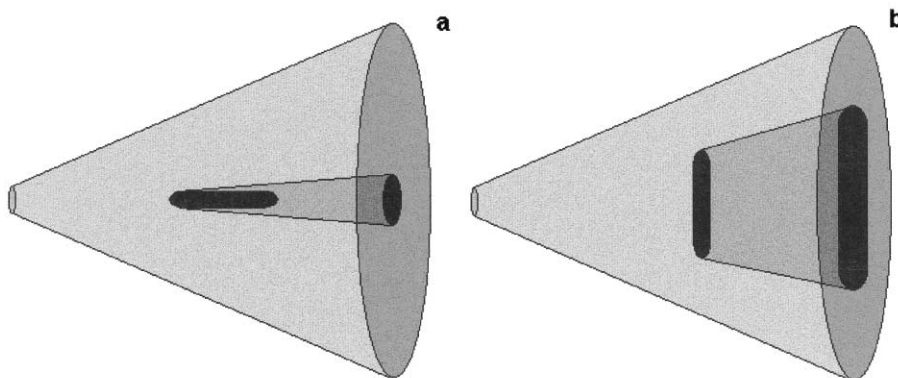


Fig. 3. Projection effect caused by an elongated particle placed in different orientations in the post-focused path.

The noise contribution that characterises the precipitant system is caused by the dynamics of particles. This can be broken down into several components.

- **Position component:** It is related to the masking capability of a particle in a focused path. The surface that can be masked by a particle depends on the position where it intercepts the path and its magnitude is a function of the ratio between R_0 and the particle size. The effect caused by a spherical particle when it is moved from nearby to remote positions of the focus is shown in Fig. 2. A significant change is observed in the projected area at the photodetector plane.
- **Morphological component:** It is only defined for non-spherical particles. It is related to the different possible orientations that a particle can take in a volume and its magnitude presents a straightforward relationship with its shape. Fig. 3 illustrates an elongated particle in two different orientations (parallel and perpendicular to the propagation axis) and the changes caused on the photodetector plane.
- **Size component:** Particles with the same morphology features, placed at the same position and orientation,

project different areas depending on their sizes, as can be observed in Fig. 4.

- **Eclipsing component:** It depends on the probabilities of the particles for masking themselves. In Fig. 5, three particles project on the photodetector plane very different areas whose surfaces depend on their relative distribution along the radial axis into the focused path.

3. Experimental

The measurements of transmittance were carried out using the device illustrated in Fig. 6, which was placed inside a dark chamber in order to minimise influences of external sources of radiation.

The precipitation tests were induced in a 4 cm inner edge cubic container made in methacrylate that was crossed by a 5 mW laser beam (He–Ne Melles Griot, model 05 LHR151), with an output wavelength of 632.8 nm. The beam was focused in the geometric centre of the reservoir with a 10 cm focal length lens, generating a hyperbolic path whose features are as follows.

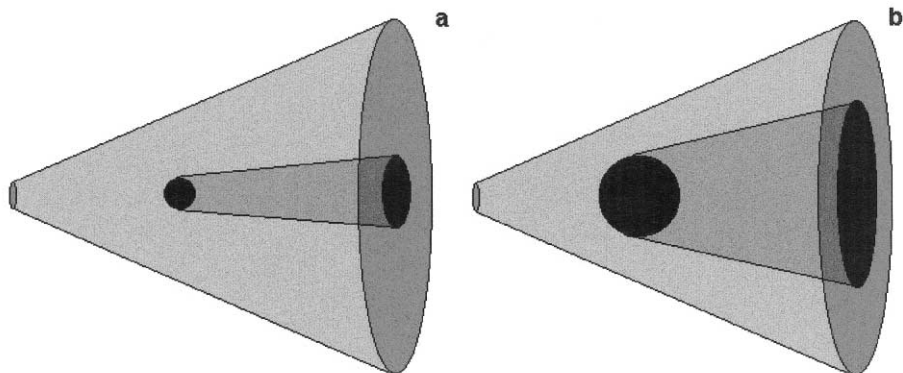


Fig. 4. Projection effect caused by spherical particles with different sizes placed in the same position in a post-focused path.

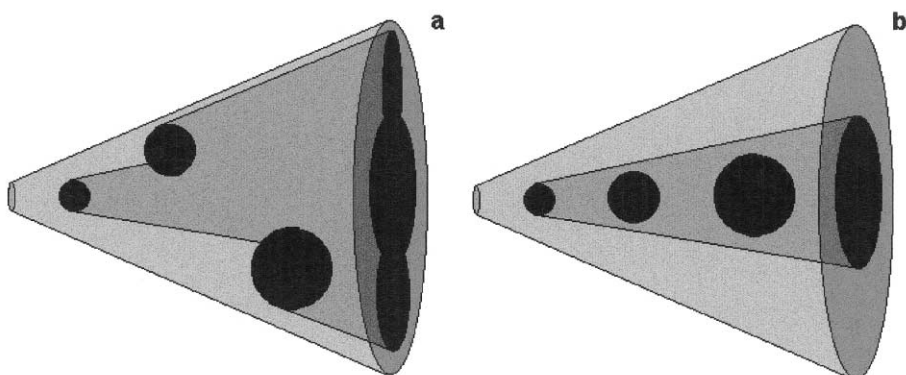


Fig. 5. Projection effect caused by spherical particles of different sizes placed in (a) different optical axes and (b) the same optical axis.

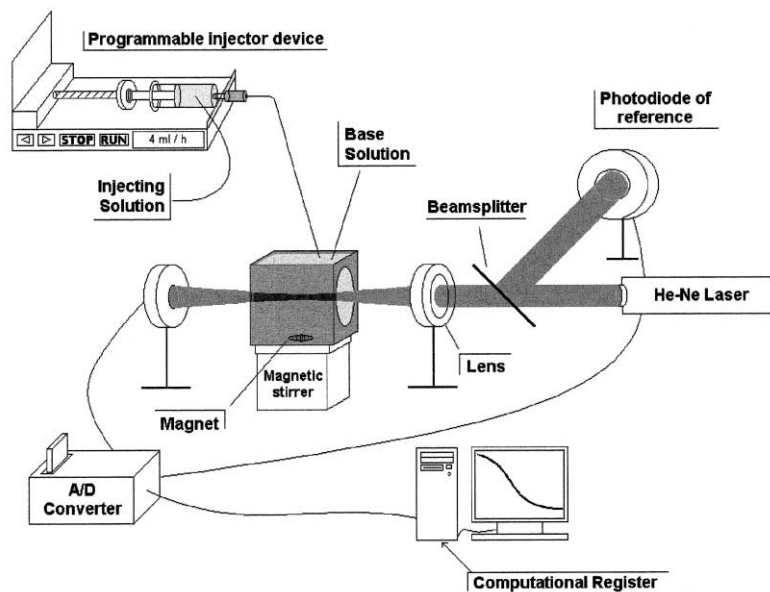


Fig. 6. Experimental device used for measuring transmittances of a precipitant system.

Table 1
Concentration ranges used in the precipitation experiments^a

Precipitated chemical	PbI ₂	PbSO ₄	BaSO ₄	BaC ₂ O ₄
K_{ps} , 25°C	8.49E-9	1.82E-8	1.07E-10	1.60E-7
Base Solution	KI	K ₂ SO ₄	K ₂ SO ₄	K ₂ C ₂ O ₄
[Concentration (M)]	0.07	0.05	0.05	0.08
Injected solution	Pb(NO ₃) ₂	Pb(NO ₃) ₂	Ba(NO ₃) ₂	Ba(NO ₃) ₂
[Range of concentrations (M)]	0.109–0.217	0.165–0.330	0.214–0.429	0.222–0.444

^a Solubility products of the generated precipitates are also indicated.

Prefocused radius (r / μm)	400
Radius at the focus (R_0 / μm)	50
Radius at the container window (R_w / μm)	95

A beam-splitter was placed between the reservoir and the laser device, so that the split beam was used as reference of the laser stability. The transmitted and the reference radiation were measured by two photodiodes THORLABS, model S20MM, with analogue output that were digitised by an autonomous system DATATAKER, model DT50, with a RS232 connection to a PC.

The whole of the system was kept without thermostating but with little thermal variations between 22.5 and 25.5°C.

In the tests carried out with that equipment, precipitated particles were generated using an injection technique where an inducing solution was added over a base one.

Concentrations of both solutions were high enough, so that the ionic concentration product (ICP) was widely exceeded when they came into contact, favouring, that way, a nucleation process against a growth process.

The inducing solution was added using a programmable injector Cole-Parmer, model 74 900, with a flow rate of $1.15 \times 10^{-3} \text{ cm}^3 \text{ s}^{-1}$ and the precipitated particles were kept in suspension with a magnetic stirrer.

In all the tests 60 cm³ of base solution and 2 cm³ of the injected one were used. The range of their concentrations were those required for the generation of 20.0, 17.5, 15.0, 12.5 and 10.0 mg of precipitation, as detailed in Table 1.

3.1. Calculation of the noise associated to the transmittance signal

The calculation of the noise associated to the transmittance signal has been obtained with a computer

application programmed in LABVIEW™ 5.0¹. Using data of temporal evolution of transmittances measured by the photodetectors (Fig. 7a), this program works with a subset of an odd number of consecutive data (C), (Fig. 7b), that are fitted to a 3rd order polynomial (Fig. 7c).

The noise is calculated by the mean squared error parameter function defined as

$$\text{Noise} = \sqrt{\frac{1}{(ne - ns)} \sum_{ns}^{ne} (TE_i - TC_i)^2} \quad (4)$$

where ns and ne are the places occupied by the initial and the final data in the experimental sequence of transmittances of the subset, TE_i is the i th data of experimental transmittance and TC_i is the i th data of transmittance calculated with the fitted polynomial.

The calculated noise is assigned to the central value of transmittance in the subset. Then the subset moves forward, taking the next data of transmittance and leaving out the first one, in such a way that the new subset takes from the data number $ns + 1$ to the $ne + 1$. Finally, the pairs of transmittance and noise obtained along the whole set generate a new graph, which characterises the precipitation process (Fig. 7d). The flowchart of the program is shown in Fig. 8.

4. Results and discussion

The variations of the transmittances measured over a period of 29 min of injection are shown in Fig. 9.

It is observed that curves of transmittance trace different plots for every chemical. However, in the curves for the same precipitate, we find some similarities, so that, the minimum transmittances are proportional to the final precipitated mass (Table 2).

The variations of transmittances in every test show the particular nucleation conditions of each chemical. In the PbI₂ curves, the initial stages in the injection process are characterised by strong changes in the transmittances and strong descent slopes, whereas, in the same period of time, the generation of PbSO₄ precipitates, takes place slowly and without abruptness. An intermediate behaviour can be observed in the case

¹ Copy registered by Centro de Cálculo. Universidad de Cádiz (UCA).

of the very similar curves generated by precipitates of BaSO_4 and BaC_2O_4 , showing mean slopes characterised by the absence of strong variations in the initial stages.

In the tests carried out with PbI_2 in quantities smaller than 20 mg, phenomena of increase of the transmittance in the final stages of the process are clearly observed. This tendency which was observed as well in PbSO_4 tests, although to a lesser extent, could be a consequence of the presence of growth processes that would compete with nucleation, (the favoured process in the first stages).

The morphological analyses of precipitates carried out with Image Tool© software (Wolcox et al., 1995–96) show the presence of flat crystals of PbI_2 and PbSO_4 at different levels of growth (Table 3 and Fig. 10). This fact supports the hypothesis of the existence of crystal growth processes of increasing influence against nucleation.

The variations of the transmittance caused by BaSO_4 and BaC_2O_4 precipitates, present very similar plots in which the increments of transmittance shown in the PbI_2 and PbSO_4 graphs can not be distinguished. In

these cases, the morphological analyses show that the size of the particles are very similar, with elongated shapes which do not present flat surfaces that could favour growth processes.

In Fig. 11, mean transmittances versus associated noises are plotted. They have been obtained by application of the program for calculating noises, using an odd parameter for the subset (C), of 151 data from a total number of 6195. The numerical information related to the position of the maximums reached in these graphs is listed in Table 4.

The highest absolute levels of noise correspond to the PbI_2 and PbSO_4 tests, in which the re-increase of the noise in the last stages is dependent on the presence of growth processes. The curves generated by the BaSO_4 and BaC_2O_4 precipitates carry less noise and the maximums reached are of the same numerical order, which is justified in relation to morphological and size similarities between the precipitated particles.

For the same chemical, curves show similar tendencies, reaching maximum noises of the same numerical order. In general terms these curves are characterised

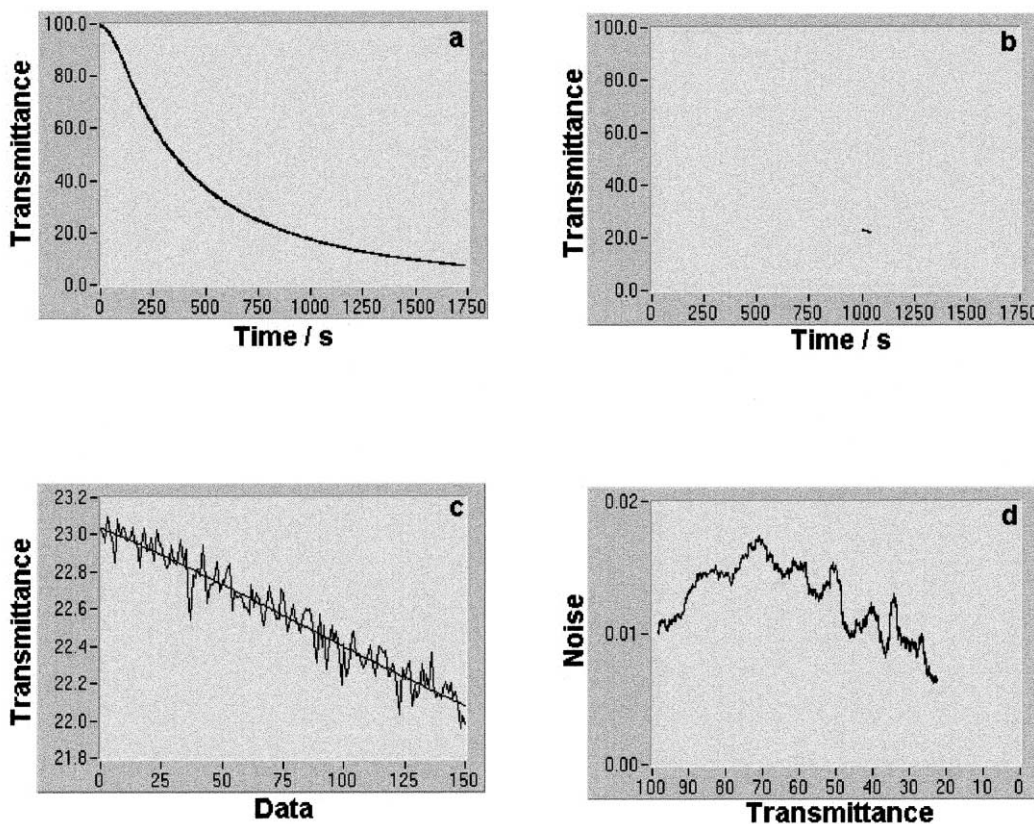


Fig. 7. Screens generated by the noise-computing program. Experimental transmittances are plotted in (a). The shifting of the subset data is shown in (b). The experimental subset data and the fitted polynomial are compared in (c). Finally, calculated noises versus calculated mean transmittances are displayed in (d).

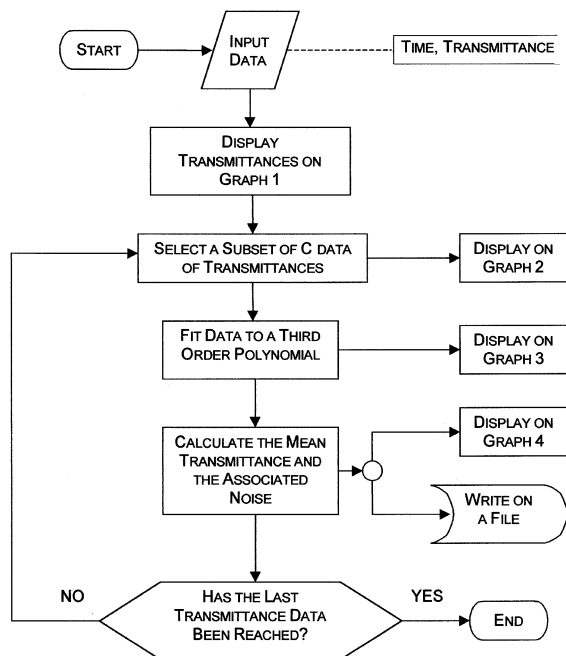


Fig. 8. Flowchart of the program designed to calculate the noise associated to the transmittance.

by: a first section where the noise increases from initial high transmittances values to transmittances where maximum noises are reached; a second section where noise decreases from medium to minimum transmittances.

For BaSO_4 experiments, only the precipitation tests which involved 20.0 and 17.5 mg of precipitate, are in accordance with the pattern curve. The other test curves of this chemical and also those concerning to PbSO_4 tests show an initial section with a similar pattern to the specified for the general cases and a second with an increase of noise, very large for PbSO_4 tests.

5. Conclusions

The use of a focused laser beam in the precipitation tests carried out with the described injection technique, constitutes a key feature to evaluate the noise associated to the transmittance, because the size of both particles and focus are of the same order.

The results of the morphological analysis reveal the relationship established between the noise of the transmittance signal and the microscopic nature of the precipitated particles in terms of size, number and morphology.

Table 2

Data of minimum (T_M) and final (T_F) transmittances after 29 min of injection corresponding to the four different chemicals and their precipitated mass

Precipitated chemical	Transmittance	Precipitated mass (mg)				
		20.0	17.5	15.0	12.5	10.0
PbI_2	T_M	1.46	8.62	13.62	15.62	29.75
	T_F	3.21	18.85	21.35	27.17	33.94
PbSO_4	T_M	55.79	60.48	66.50	68.86	72.83
	T_F	56.19	63.74	68.03	69.92	74.87
BaSO_4	T_M	7.43	9.88	21.27	21.83	31.74
	T_F	7.58	9.98	21.64	22.35	32.69
BaC_2O_4	T_M	7.51	8.46	9.96	12.15	21.93
	T_F	7.56	8.67	10.26	12.24	22.12

Table 3

Size and morphology data extracted by using image analysis software^a

Precipitated chemical	Mean size (μm)	Standard deviation (μm)	Crystallographic morphology
PbI_2	11.4	3.4	Hexagonal
PbSO_4	6.0	1.7	Rhombic
BaSO_4	6.3	1.8	Rhombic
BaC_2O_4	5.6	1.4	–

^a Measurements were obtained by using samples of 50 precipitated particles for each chemical.

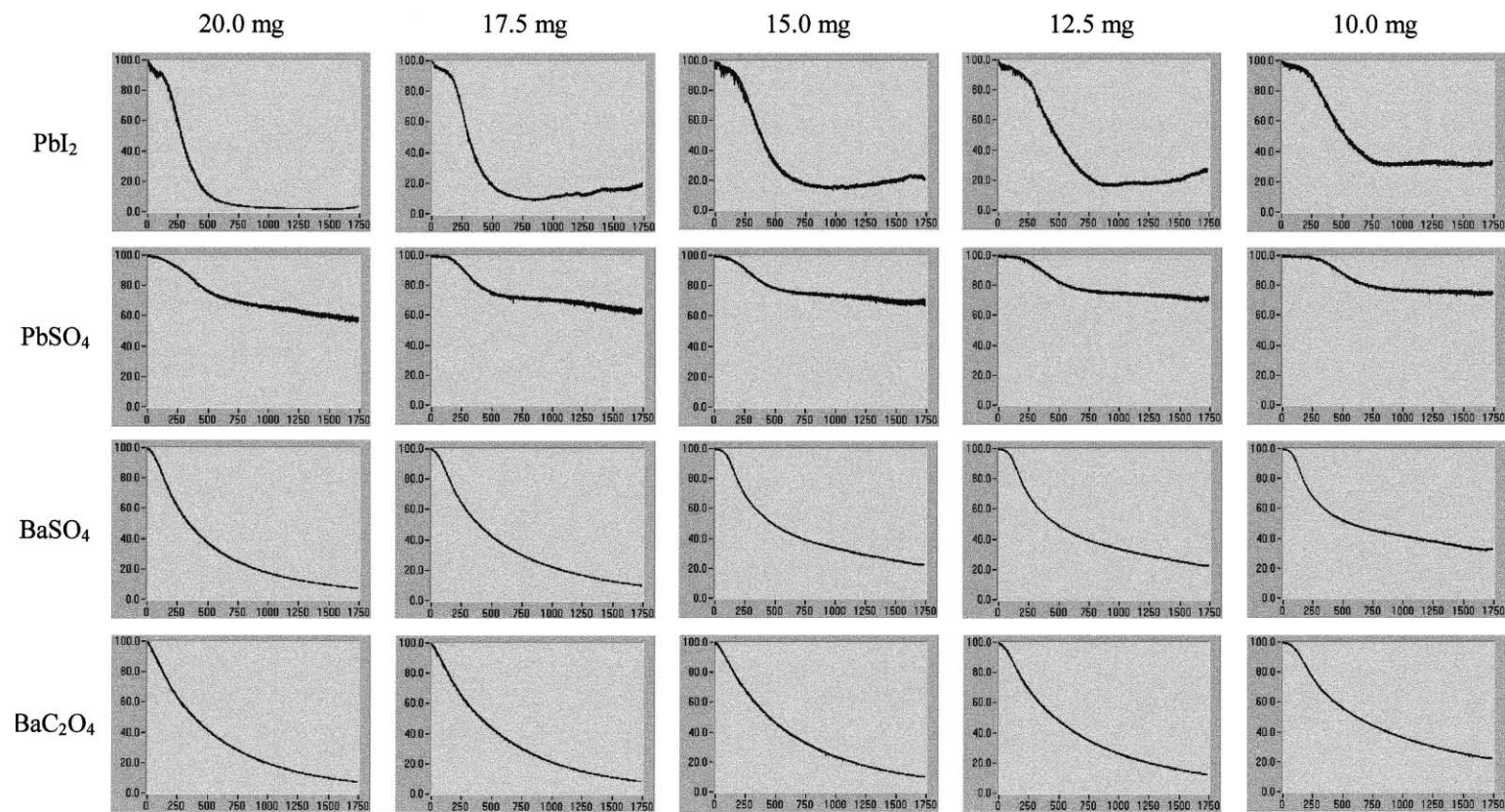


Fig. 9. Time variations of transmittances in different precipitant systems.

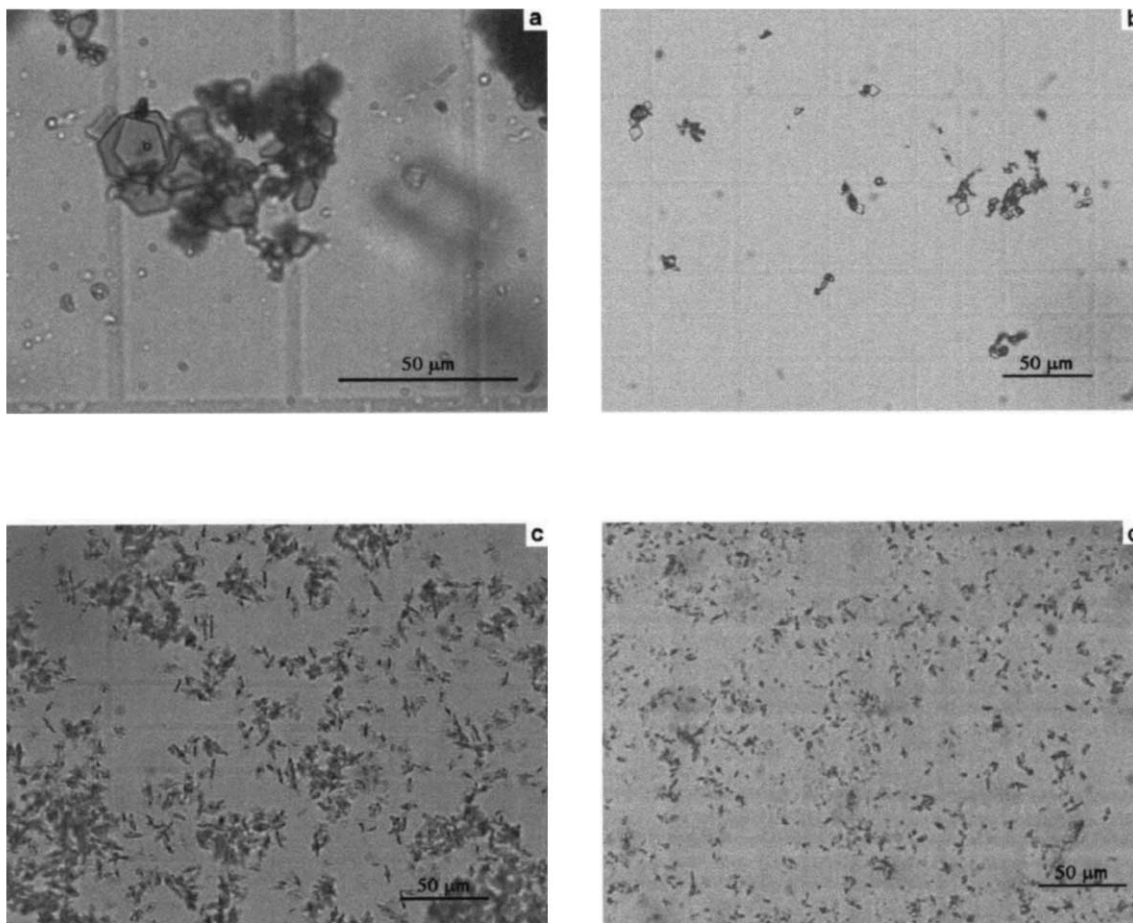


Fig. 10. Pictures of precipitated particles obtained by using light microscopy: (a) PbI_2 ; (b) PbSO_4 ; (c) BaSO_4 ; (d) BaC_2O_4 .

Table 4

Data corresponding to the maximum noise point in the curves of transmittance that are plotted in Fig. 10.

Precipitated chemical	Data of the maximum noise point	Precipitated quantity (mg)				
		20.0	17.5	15.0	12.5	10.0
PbI_2	Transmittance	64.80	55.66	89.20	95.89	61.06
	Noise	0.089	0.061	0.114	0.080	0.077
PbSO_4	Transmittance	58.28	63.06	69.32	71.04	74.70
	Noise	0.064	0.069	0.069	0.054	0.051
PbSO_4	Transmittance	61.26	74.64	74.43	86.55	32.72
	Noise	0.029	0.019	0.014	0.014	0.019
BaC_2O_4	Transmittance	89.19	86.04	72.34	72.06	24.50
	Noise	0.033	0.034	0.025	0.026	0.016

Therefore, the similar numerical order found in the maximum noises for the tests performed for every chemical, entails the presence of a relationship between noise and shape of precipitated particles.

The increasing influence of growth processes, favoured

by the presence of flat particles at the final stages of the precipitation processes, would explain the retrace of the curves of transmittance in the PbI_2 and PbSO_4 tests.

On the whole, the generation and evolution of the precipitated particles in a homogeneous liquid medium,

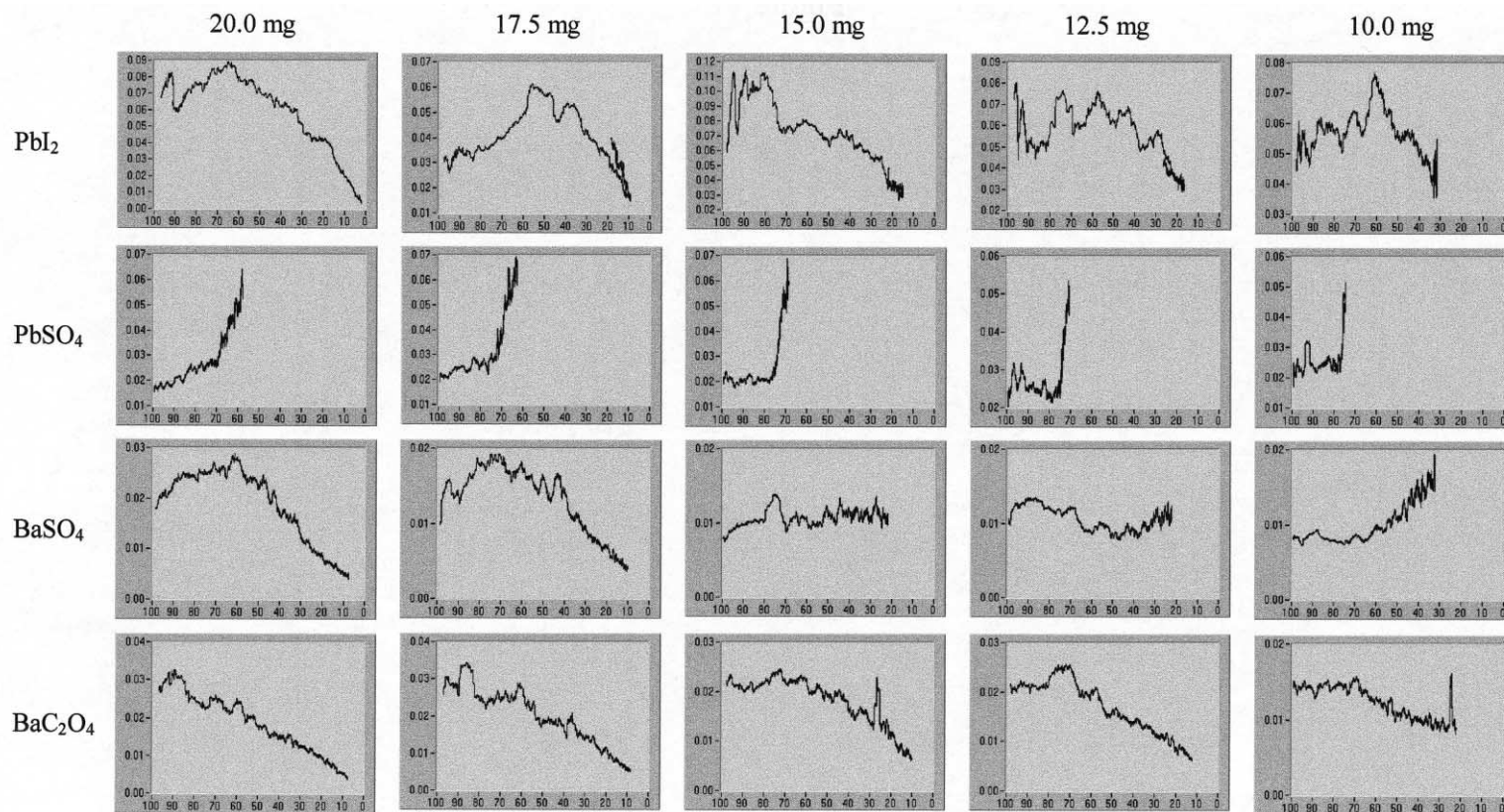


Fig. 11. Charts of noises versus transmittances measured for the four different chemicals.

carries a progressive decrease of the transmittance whose noise is in agreement with the different noise components (position, morphological, size and eclipsing) described in the theoretical section.

We can conclude that a focused laser beam is a useful tool for evaluating noises associated to transmittances in precipitant systems, whose values contain not only information about the microscopic properties of the precipitates, but also about the evolution of nucleation and growth processes. All this suggests that, the methodology used in this research is a suitable technique for the study of the nature of precipitation processes.

Acknowledgements

This work was supported by the Spanish DGICYT under Grant ALI97-0885.

References

- Burger, T., Ploss, H.J., Kuhn, J., Ebel, S., Fricke, J., 1997. *Appl. Spectrosc.* 51 (9), 1323.
- Carton, A., Marcos, M.M., Sobrón, F., Bolado, S., 1999. *Inf. Technol.* 10 (1), 173.
- Gerrard A., Burch J.M., 1994. *Introduction to Matrix Methods in Optics*, Dover Publications. New York.
- Martín, J., Alcántara, R., García-Ruiz, J.M., 1991. *Cryst. Res. Technol.* 26, 35.
- Martín, J., García-Ruiz, J.M., Alcántara, R., 1992. *Cryst. Res. Technol.* 27, 799.
- Matthews, H.B., Rawlings, J.B., 1998. *AICHE J.* 44 (5), 1119.
- Mucha, M., Ganicz, T., 1996. *J. Therm. Anal.* 46 (3–4), 795.
- Ohshima, N., 1996. *J. Appl. Phys.* 79 (11), 8357.
- Wolcox D., Dove B., McDavid D., Greer D. 1995–96. *Image tools*, V.2.0, © The University of Texas Health Science Center in San Antonio UTHSCSA.